Smooth Blending of Two Inks of Similar Hue to Simulate One Ink

Mark Shaw*, Raja Bala**, Gaurav Sharma***
*Hewlett-Packard Company, 11311 Chinden Blvd, MS227-2U, Boise, Idaho 83714
**Xerox Innovation Group, 800 Phillips Rd, 128-27E, Webster, NY 14580
***ECE Dept, RC Box 270126, University of Rochester, Rochester, NY 14627-0126

ABSTRACT

The use of four process inks (CMYK) is common practice in the graphic arts, and provides the foundation for many output device technologies. In commercial applications the number of inks are sometimes extended beyond the process inks depending on the customers' requirements, and cost constraints. In inkjet printing extra inks have been used to both extend the color gamut, and/or improve the image quality in the highlight regions by using "light" inks. The addition of "light" inks are sometimes treated as an extension of the existing Cyan or Magenta inks, with the Cyan tone scale smoothly transitioning from the light to the dark ink as the required density increases, or are sometimes treated independently.

If one is to treat the light ink as an extension of the dark ink, a simple blend can work well where the light and dark inks fall at the same hue angle, but will exhibit problems if the light and dark inks hues deviate significantly. The method documented in this paper addresses the problem where the hues of the light and dark inks are significantly different. An ink interaction model is built for the light and dark inks, then a composite primary is constructed that smoothly transitions from the light ink to dark ink, preventing the blended ink from over inking, while ensuring a smooth transition in lightness, chroma, and hue.

The method was developed and tested on an XES (Xerox Engineering Systems) ColorGraphx X2 printer, on multiple substrates, and found to provide superior results to the alternative linear blending techniques.

1. INTRODUCTION

Color ink jet printing has developed with the use of more than four colored inks. Typically the increased number of inks is designed to perform one of two major functions. In some cases the use of extra primaries increases the color gamut of the printer, allowing the reproduction of colors previously unattainable. A primary example of this is Hi-Fi Color[1]. Alternatively, the extra primaries have been used to improve the image quality of the existing ink set by providing additional ink of higher lightness and of similar hue. The lighter ink appears less grainy to the observer and therefore renders highlight details more smoothly. This is particularly advantageous in reproduction of skin tones where the grainy appearance is a serious source of customer dissatisfaction.

In some cases the lighter ink may yield a ramp[†] of the same hue as that of the dark ink, but this is not always the case. Sometimes the light ink has a different hue even though the same dye or pigment is used. One may postulate that the differences are due to the non-linear interactions of light, solvent, dye or pigment, and paper, and often produces a primary of different hue angle. An example of this can be seen in Figure 1, where ramps of light and dark inks printed on a ColorGraphx X2 wide-format inkjet printer are measured and plotted in 3-D CIELAB space. From the plots it is apparent that the light and dark inks have significant differences in their hue angle.

[†] We will refer to single colorant prints that range from zero to one-hundred percent in coverage as a ramp for the colorant.

Color Imaging X: Processing, Hardcopy, and Applications, edited by Reiner Eschbach, Gabriel G. Marcu,
Proc. of SPIE-IS&T Electronic Imaging, SPIE Vol. 5667 © 2005 SPIE and IS&T · 0277-786X/05/$15

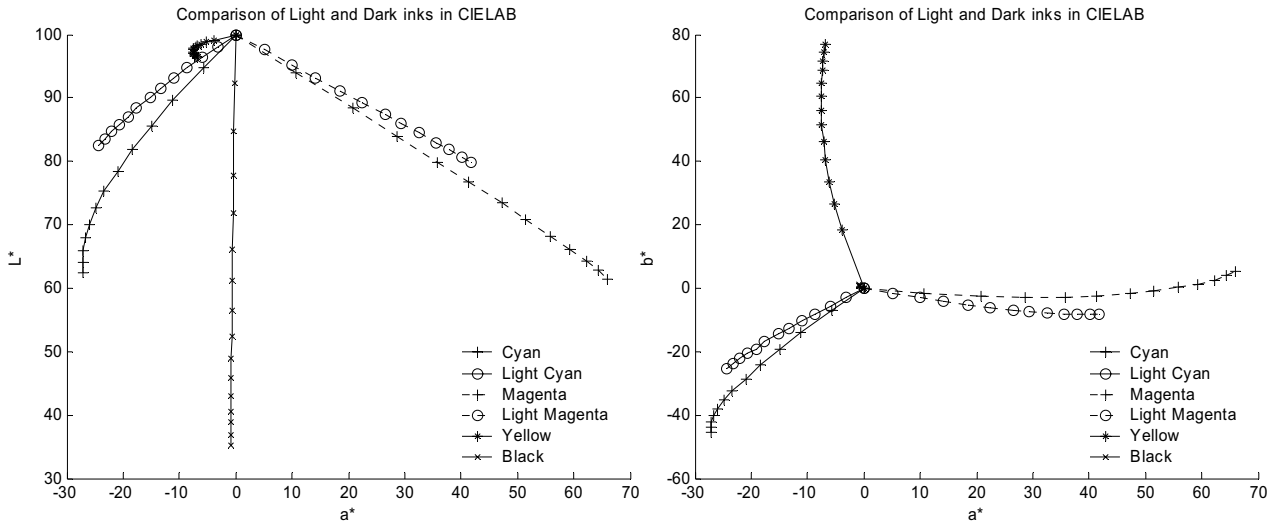

Figure 1 : (Left) CIELAB a*b* Projection of the ColorGraphx X2 CMYK Lc Lm inks
(Right) CIELAB L*a* Projection of the ColorGraphx X2 CMYK Lc Lm inks

Existing approaches to blending light and dark inks of the same type have typically taken the form of two, piecewise linear functions that have pre-defined shape and form[2]. An example of such is shown in Figure 2, whereby the blending function is controlled by six numbers that specify the start, mid, and end points for both the Light and Dark inks. The x-axis of this plot can be thought of as the effective colorant amount as a result of the blending of light and dark inks. Once the blending is performed the printer may be addressed in terms of this effective colorant amount and a ramp of this effective colorant corresponds to blends of the two colorants in the amounts shown in Fig 2. Further color characterization[3] can then address the printer in terms of these effective colorants.

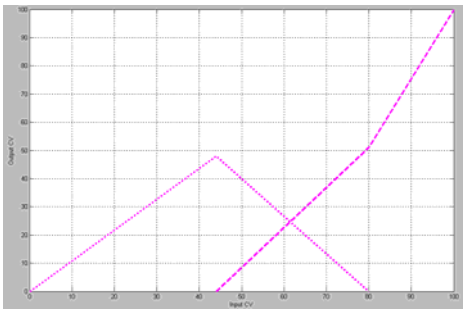

Figure 2 : Light and Dark blending function used by an Existing Printer. Light (..) and Dark (--) Magenta Light and Dark Cyan functions are identical

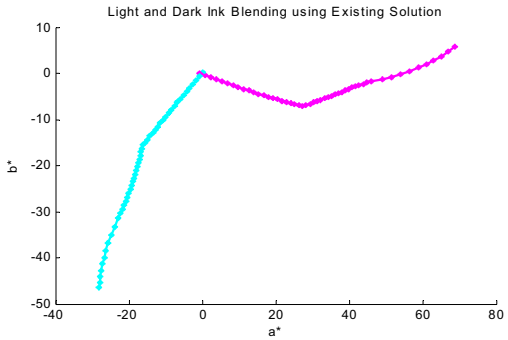

Figure 3 : CIELAB a*b* plot of the hue transition using the linear blend in Figure 2

This approach can work well when the hues of both the light and dark inks are aligned. Unfortunately, when the light and dark ink hues are not aligned, the blended tone curve can result in a sharp change in hue from the light to the dark ink. Figure 3 illustrates this problem for the printer whose individual colorant ramps were shown in Figure 1. Use of the piecewise linear blending functions of Fig. 2 yields effective Cyan and Magenta colorants whose location in the CIELAB a*-b* plane are shown in Figure 3. Sharp transitions in hue can be seen in the hues of the effective cyan and magenta colorants. These sharp transitions can cause a severe strain on the subsequent color characterization which typically assumes a smooth behavior and therefore results in significantly higher errors in color management upstream of the blending.

2. PROPOSED ALGORITHM FOR INK BLENDING

This paper describes an algorithm that automatically builds a smooth transition function between the light to dark inks. The algorithm is designed to maintain smooth transitions in Lightness, Chroma, and Hue. The steps are as follows:

1. A relationship between digital code value (CV) sent to the printer and chroma weighted Delta E from paper (CDE) are determined for both Light and Dark inks. The chroma weighted Delta E from paper metric was found to be a more effective method for weighting than some more commonly used metrics such as (ΔE_{ab} or ΔE_{94} color difference equations[4]), providing more information at high chroma regions where maximal chroma is desired. The following equation was used to compute the metric.

$$CDE_i = \sqrt{(L_{wt} - L_i)^2 + (a_{wt} - a_i)^2 + (b_{wt} - b_i)^2)} * \sqrt{a_i^2 + b_i^2}$$

$$Lab_{wt} = \text{CIELAB of media white point}$$
$$Lab_i = \text{CIELAB of sample} \qquad (1)$$

The CV vs CDE relationship is used to determine the point at which the maximum print density of each ink has been reached (DMax). At this point, the addition of more ink does not make the print any darker, so it is determined as the channel's ink limit threshold. This CV-CDE relationship is also used to linearize the printer response from the minimum density (i.e. paper) to the maximum density for each of the inks. The transform is stored as a 1-dimensional CV-to-CDE lookup table (LUT), which will be used later in the algorithm. Figure 4 illustrates the behavior of a typical set of inks on the Colorgraphx X2.

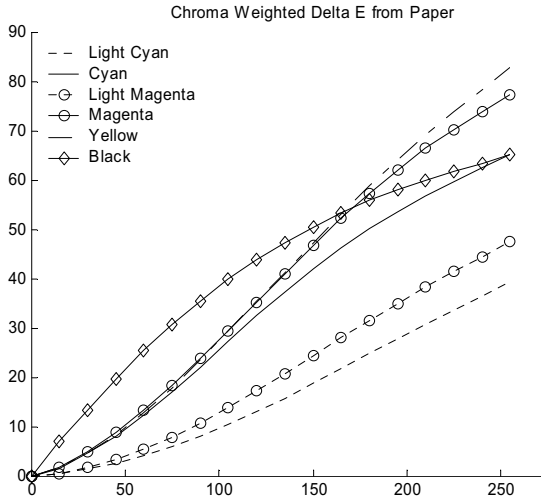

Figure 4 : Chroma Weighted Delta E response of CMYKLcLm Inks

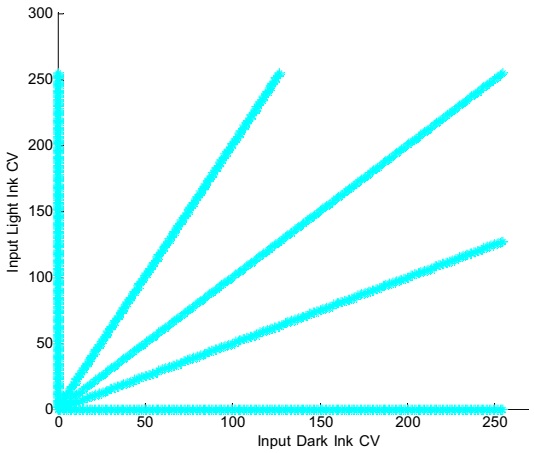

Figure 5 : Sampling of light and dark ink interactions

2. A set of patches are then printed that sample the interaction of both light and dark inks. The printed patches include a ramp of pure light ink, a ramp of pure dark ink, a ramp of light and dark ink of equal code values, a ramp of light ink and dark ink where the code values of the light ink are half that of the dark ink, and a ramp of dark ink and light ink where the code values of the dark ink are half that of the light ink. The assumption is made that the ramp is sampled from DMin to DMax in linear increments in both inks, where DMin and DMax denote the minimum density and maximum density, respectively.

An example of this is shown in Figure 5, where the interactions of the light and dark inks are being sampled using five vectors in the two dimensional space.

3. The patch data are measured using a spectrophotometer, and Principal Component Analysis is used to relate the spectral characteristics of the patches to the input code values requested using the following procedure :

i. Assuming a Beer's Law[5] like behavior, the measured reflectances are normalized by dividing the reflectance of the white paper. This approach was chosen in favor of alternative methods such as Kubelka-Munk[6,7] or Neugebauer[8,9] due to simplicity.

$$R_{normalized(\lambda)} = \left(\frac{R_{measured(\lambda)}}{R_{paper(\lambda)}} \right) \tag{2}$$

ii. The patch spectral reflectances are converted to spectral densities. (Since the patches were printed in linear increments of CDE, this provides a good starting point)

$$D_{data(\lambda)} = -\log_{10}\left(R_{normalized(\lambda)}\right) \tag{3}$$

iii. Principal Component Analysis was then applied to the Light/Dark Cyan data, and Light/Dark Magenta data separately to extract the two basis vectors (in each case) that explain the largest amount of variance contained within the data. The assumption being that the first two vectors represent a smooth estimate of the spectral density characteristics of the light and dark inks.

PCA is a mathematical technique for analysis of a set of multivariate data. The technique provides a representation of the multivariate data as a linear combination of orthonormal basis vectors, wherein each successive basis vector accounts for as much of the variation in the original data as possible.[10,11] For subtractive color systems the method is particularly useful in the analysis of colorant characteristics[12].

iv. Using a 2x2 matrices (m1,m2) derived by least squares regression, we approximate the spectral density profiles of the light and dark inks in terms of the first two eigenvectors mentioned above. The resulting approximations may be interpreted as "rotations" of the eigenvectors to represent the shape and form of the spectral density profiles of the pure Light and Dark inks. The rotated vectors are shown in Figure 6.

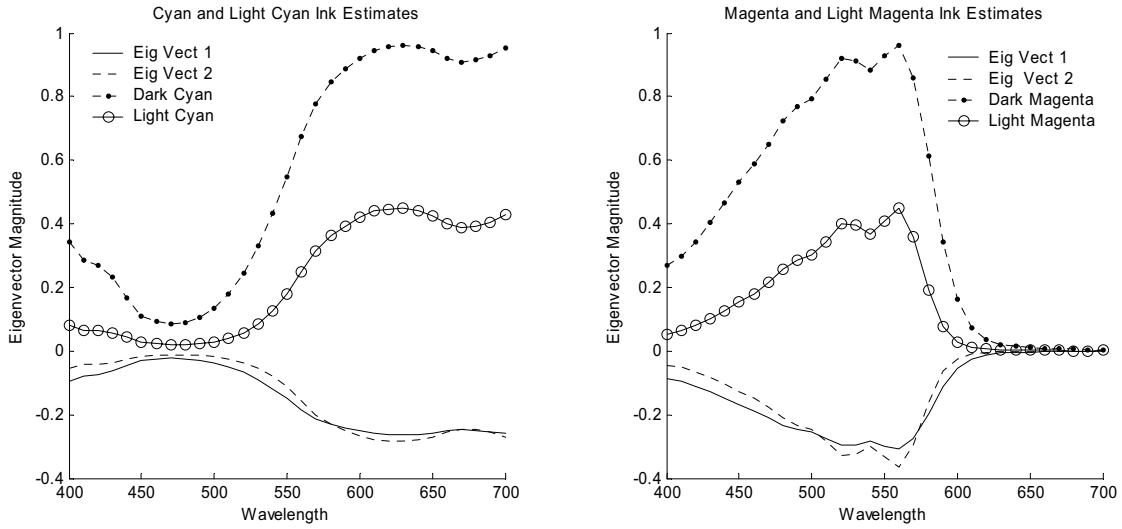

Figure 6 : Original (negative values) and rotated (positive values) basis vectors of Light and Dark inks

$$V_{cyan\_ink(\lambda)} = EV_{cyan\_ink(\lambda)} \cdot m$$
$$V_{light\_cyan\_ink(\lambda)} = EV_{light\_cyan\_ink(\lambda)} \cdot m \tag{4}$$

v. A non-linear optimization using a sequential quadratic programming (SQP) method[13] was then used to calculate the 'amount' of each of the light and dark inks (as represented by the spectral density estimates from the above process) required to reconstruct the spectral density for all measured patches. The calculations in the process are shown in Eqn.(5). For each measured patch, the iterative process estimates the values for α and β that minimize the variable *Error* in Eqn (5), where XYZ(), Lab(), and ΔE() are functions to convert from reflectance space to XYZ space, XYZ to CIELAB space, and to calculate the ΔE_{76} metric, respectively.

$$D_{recon(\lambda)} = \alpha \cdot V_{light\_cyan\_ink(\lambda)} + \beta \cdot V_{cyan\_ink(\lambda)}$$
$$R_{recon(\lambda)} = 10^{-D_{recon(\lambda)}}$$
$$Error = \Delta E(\, Lab(\, XYZ(\, R_{recon(\lambda)})),\, Lab(\, XYZ(\, R_{data(\lambda)})))\, \tag{5}$$

vi. Least squares regression is then used to derive a polynomial that relates the scalar ('amounts') of each of the inks derived in the previous step to the density linearized input code values. The polynomials contain both linear terms and non-linear terms.

$$\alpha_{lt\_cyan} = a_0 + a_1 C + a_2 Lc + a_3 C \cdot Lc + a_4 C^2 + a_5 Lc^2 + a_6 C^2 \cdot a_7 Lc^2 + a_8 C^3 + a_9 Lc^3$$
$$\beta_{cyan} = b_0 + b_1 C + b_2 Lc + b_3 C \cdot Lc + b_4 C^2 + b_5 Lc^2 + b_6 C^2 \cdot b_7 Lc^2 + b_8 C^3 + b_9 Lc^3$$
where C (Dark Cyan) and Lc (Light Cyan) are density linearized code values

$$\alpha_{lt\_magenta} = a_0 + a_1 M + a_2 Lm + a_3 M \cdot Lm + a_4 M^2 + a_5 Lm^2 + a_6 M^2 \cdot a_7 Lm^2 + a_8 M^3 + a_9 Lm^3$$
$$\beta_{magenta} = b_0 + b_1 M + b_2 Lm + b_3 M \cdot Lm + b_4 M^2 + b_5 Lm^2 + b_6 M^2 \cdot b_7 Lm^2 + b_8 M^3 + b_9 Lm^3$$
where M (Dark Magenta) and Lm (Light Magenta) are density linearized code values (6)

Figure 7 shows the model prediction of the light and dark ink interactions for a large number of input ink combinations. The density linearized input code values were converted to scalars for the spectral estimates using the polynomial, then the spectral data converted to CIELAB units. The o's represent the measured data from the light ink ramp, the *'s represent the measured data from the dark ramp, the .'s are the modeled ink combinations.

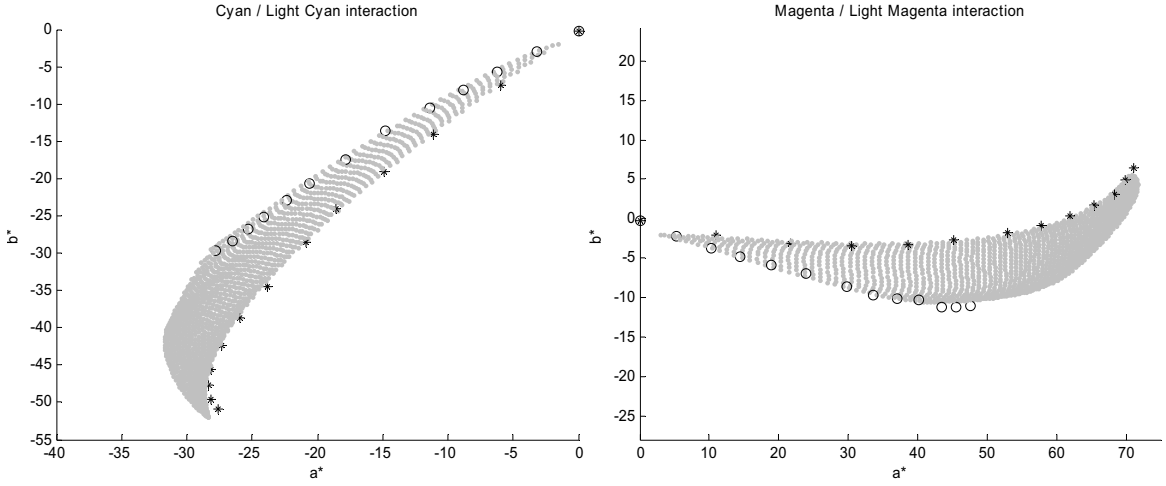

Figure 7 : CIELAB a*b* plots of model prediction of light and dark ink interactions for Cyan (Left) and Magenta (Right) inks

4. The next step is to use the model to predict the colorimetric response of any combination of light and dark inks, and build a smooth transition from the light to dark ink.

i. The first stage is to set the ink limit for the interaction of light and dark inks. Only combinations of light and dark cyan below a threshold are considered 'in gamut'. This can be seen when comparing Figures 7 and 8, where regions are missing in Figure 8 in order to avoid the problem of over-inking, which can cause serious degradation in image quality in the inkjet printers in consideration.

ii. Next a selection of points within the gamut are chosen to 'guide' the light and dark transition. These points are chosen such that only the light ink is used for the first ¼ of the curve, the dark ink is only used at the end of the curve, and some additional control points are added to adjust the mid-tone curvature of the transition. Example transition curves for Cyan and Magenta are shown in Figure 8.

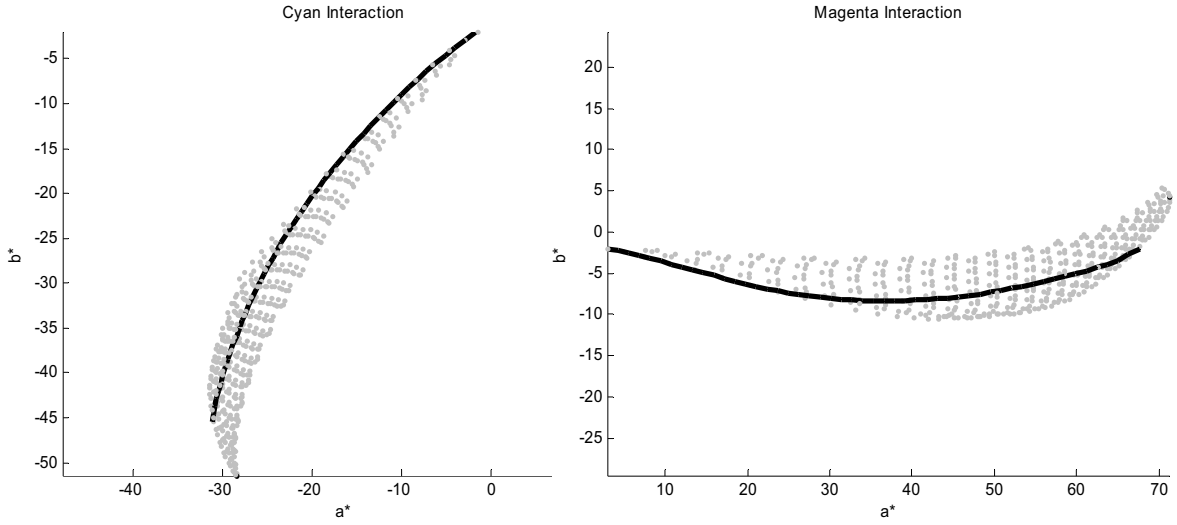

Figure 8 : CIELAB a*b* plots of the colors available when printing light and dark inks with cyan (left) and magenta (right). The line smoothly sweeping through the dots indicates the desired transition from light to dark ink.

iii. Once each ink transition curve has been chosen in CIELAB space, the model must be inverted to convert the curve to linearized density space code values.

To avoid introducing further error when inverting the polynomial, a second constrained non-linear optimization using sequential quadratic programming (SQP) performed the inversion[13]. The forward model was used to iteratively predict the most suitable linearized density space code values. The performance criteria was based on the CIE ΔE_{ab} color difference between the aim and the model predicted values.

iv. The code values are then mapped through the inverse of the original density linearization LUT, thus relating the linearized CDE values to raw printer CV's.

3. EXPERIMENTAL RESULTS AND DISCUSSION

The proposed algorithm defines a computational framework for developing a color model as to how two inks interact, and the use of this model to derive a smooth hue transition for light and dark inks of different hue.

Substrate	*Cyan*	*Magenta*
115gsm Presentation	0.833	0.400
160gsm Presentation Paper	0.317	0.317
90gsm Hi White	0.743	0.748
360 Presentation	0.795	0.549

Substrate	*Cyan*	*Magenta*
Banner Fabric	0.339	0.791
Banner Vinyl	0.331	0.455
Blue Backed Paper	0.257	0.453
Premium PSV	0.286	0.376

Table 1 – Average model prediction accuracy (ΔE_{ab}) for ink interaction models on a selection of media types.

The performance of this forward model, as demonstrated on a variety of different substrates can be seen in Table 1. The results show the mean color difference of the measurements used to train the forward model, compared to the model prediction. The substrate types varied significantly from low grade un-calendared to high grade synthetic materials. The model performed well in all cases, and the results were successfully used in the development of color-tables for the XES ColorGraphx X2 printer. The final blending of light and dark inks using the 1D LUTs is shown in Figure 9.

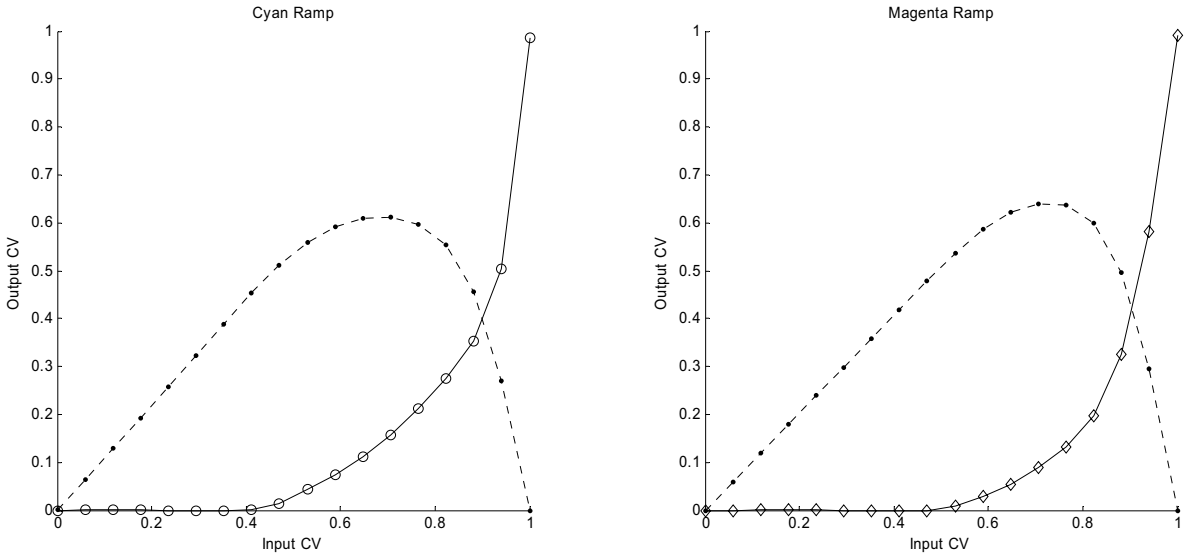

Figure 9 : Final interaction TRCs for Cyan and Magenta inks
solid lines are the light inks, ++'s are the dark inks

Instead of using a polynomial model, the authors also used trihedral (i.e. 2-D triangular) interpolation to develop the forward model. Both models worked well, but the trihedral interpolation suffered from non-monotonic behavior when the optical density of the inks reaches its asymptotic level. In retrospect, those problems could have been averted if the data were properly pre-conditioned prior to the interpolation.

4. CONCLUSION

We present a method for the blending of two inks of similar hue in printers using light and dark ink combinations of "same color". The method offers a significant improvement over existing piece-wise linear blending approaches in printers where the light and dark inks show significant hue differences. In such printers, while existing blending methods introduce sharp transitions, the proposed method produces smooth responses for the blended inks. This reduces the strain on color characterization and thereby improves the accuracy of characterization. The method has been successfully implemented on an inkjet printer where test results confirm its performance advantages.

5. ACKNOWLEDGEMENTS

The authors would like to thank George Tsang and Frank Shah of Xerox Engineering Systems for the support of this work.

6. REFERENCES

1. H. Kueppers, *US Patent 4812899*, issued March 14, 1989.
2. Y. X. Nayes, J. Y. Hardeberg, and A. M. Moskalevm *Linearization Curve Generation for CcMmYK Printing*, IS&T Eighth Color Imaging Conference, November 2001. pp. 247-251.
3. R. Bala, *Device Characterization*, Chapter 5 of Digital Color Imaging Handbook, Gaurav Sharma Ed., CRC Press, Boca Raton, FL, 2003.
4 CIE publication No. 116-1995, *Industrial color difference evaluation,* Central Bureau of the CIE, Vienna, 1995.
5 Billmeyer FW, Saltzman M. *Principles of Color Technology*, Second Edition, John Wiley & Sons, New York, 1981.
6 Allen E, *Colorant Formulation and Shading in Optical Radiation Measurement Vol. 2 Color Measurement*, Gram F and Bartleson CJ (eds.), Academic Press, New York, 1980.
7 Judd DB, Wyszecki G. *Color in Business, Science and Industry*, John Wiley & Sons, Inc., New York, 1975.
8 Yule JAC. "Principles of Color Reproduction", John Wiley & Sons, New York, 1967.
9 Balasubramanian R, *Optimization of the Spectral Neugebauer Model for Printer Characterization*, J Elec Imag 1999;8:156–166.
10 Reachner AC, *Methods of Multivariate Analysis,* John Wiley & Sons, New York, 1995.
11 Golub GH, Van Loan CF, *Matrix Computations,* Second Ed., 1989, The Johns Hopkins University Press, Baltimore, MD
12 G. Sharma, *Set theoretic estimation for problems in subtractive color,* Color Res. Appl., vol. 25, no. 4, pp. 333-348, October 2000.
13 Schittkowski, K., *NLQPL: A FORTRAN-Subroutine Solving Constrained Nonlinear Programming Problems,* Annals of Operations Research, Vol. 5, pp 485-500, 1985